ACS APPLIED MATERIALS & INTERFACES

Research Article

www.acsami.org

Crack-Free and Scalable Transfer of Carbon Nanotube Arrays into Flexible and Highly Thermal Conductive Composite Film

Miao Wang,[†,‡] Hongyuan Chen,[‡] Wei Lin,[‡] Zhuo Li,[§] Qiang Li,*[,†] Minghai Chen,*[,‡] Fancheng Meng,[‡] Yajuan Xing,[‡] Yagang Yao,*[,‡,§] Ching-ping Wong,[§,∥] and Qingwen Li[‡]

[†]School of Power and Energy Engineering, Nanjing University of Science and Technology, Nanjing 210094, China

[‡]Suzhou Institute of Nano-tech and Nano-bionics, Chinese Academy of Sciences, Suzhou 215123, China

[§]School of Materials Science and Engineering, Georgia Institute of Technology, 771 Ferst Drive, Atlanta 30332, United States

[∥]Department of Electronic Engineering, Faculty of Engineering, The Chinese University of Hong Kong, ShaTin, Hong Kong

Supporting Information

ABSTRACT: Carbon nanotube (CNT) arrays show great promise in developing anisotropic thermal conductive composites for efficiently dissipating heat from high-power devices along thickness direction. However, CNT arrays are always grown on some substrates and liable to be deformed and broken into pieces during transfer and solution treatment. In the present study, we intentionally synthesized well-crystallized and large-diameter (~80 nm) multiwalled CNT (MWCNT) arrays by floating catalyst chemical vapor deposition (FCCVD) method. Such arrays provided high packing density and robust structure from collapse and crack formation during post solution treatment and therefore favored to maintain original thermal and electrical conductive paths. Under optimized condition, the CNT arrays can be transferred into flexible composite films. Furthermore, the composite film also exhibited excellent thermal conductivity at 8.2 W/(m·K) along thickness direction. Such robust, flexible, and highly thermal conductive composite film may enable some prospective applications in advanced thermal management.

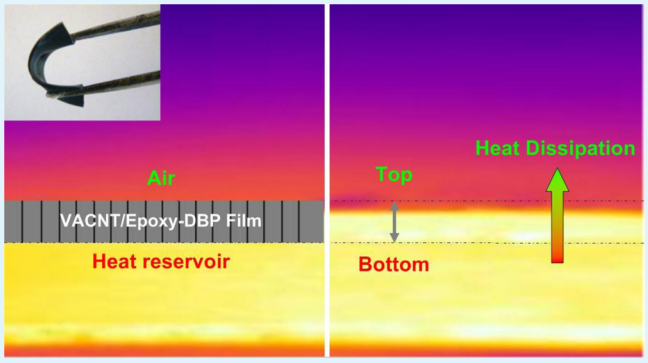

KEYWORDS: *carbon nanotube array, crack-free, scalable transfer, flexible, highly thermal conductive*

1. INTRODUCTION

Among graphite family, carbon nanotubes (CNTs) have been viewed as one of most promising candidates for the development of robust and highly thermal conductive films for heat dissipation in high-power devices.[1−3] It has been well investigated that the thermal conductivity in axial direction for individual CNTs can be as high as 3000 W/(m·K), and reach at 6000 W/(m·K) for structurally perfect single-walled carbon nanotubes (SWCNTs).[4−7] Hence, CNT powder was once mixed with polymers to enhance its thermal conducting performance.[8−11] However, the limited improvement was observed for the random CNT network with low volume fraction and poor contact with each other in the resulting composites.[12−16] In addition, when the CNTs are processed into macroscale films, for instance, CNT buckypaper,[17−21] which can be prepared by the vacuum filtration of CNT dispersion, typically presents its thermal conductivity around a couple of hundreds of W/(m·K) in plane direction but <5 W/(m·K) along thickness direction.[22,23] The formation of cross-plane porous network and poor interfacial contacts between the intertubes are key factor for the dramatic decrease of thermal conductivity in thickness direction. As a result, densely aligned CNT structure is ideal scaffold for bridging the CNT performance from nanoscale to macroscale.

As such, vertical aligned CNT (VACNT) arrays represent superior thermal conductive performance than other carbon nanotube macroscale films in thickness directions, thus could be a promising candidate for high-performance thermal interface materials (TIMs) in high-power devices.[24−27] The thermal conductivity of thin-layer CNT arrays are often ~60 W/(m·K) along the alignment direction tested by the laser flash method.[28−31] But it is difficult to prepare large area freestanding VACNT films without substrate, which limits their practical applications; to address these problems, attempts were reported to infuse polymer into VACNT film to prepare a freestanding composite film. The introduction of polymer could reinforce the VACNT scaffold while cannot maintain a high thermal conductivity of VACNT, due to the significant self-shrinkage and damage to the ideal aligned structure in composite process, and the ultralow volume fraction of VACNT.[32−40] Then, how to transfer the CNT arrays to be a

Received: October 18, 2013
Accepted: December 10, 2013
Published: December 10, 2013

robust film while maintain the structural integrity and the highly thermal conductivity has been a key issue to their further applications. As generally reported, VACNTs have CNT volume fraction of lower than 5%, thus increasing the volume fraction of CNTs in their composites has been the critical point.[34,41] Furthermore, many original crystal defects in as-prepared CNT arrays could also largely limit their thermal conductivity.[42]

In this study, large-diameter and well-crystallized multiwalled CNT (MWCNTs) arrays were fabricated with thermal conductivity of 17.8 W/(m·K) in thickness direction (the diameter of individual MWCNTs was approximately 80 nm and the density of the arrays was 0.17 g/cm^3, Supporting Information Figure S1). Epoxy was infiltrated into VACNT to prepare a VACNT/Epoxy composite film for its favorable interface compatibility with CNTs. The thermal conductivity of composite film in its thickness direction could be 13.2 W/(m·K). It has extremely maintained the thermal conductivity of VACNT by 74.6%, which is much higher than traditional CNT array composites.[32−34] The large diameter of MWCNTs in arrays provide high density and strong structure from collapse in composing to keep the original ideal thermal paths. MWCNT arrays with large diameter avoid shrinkage in solution and thus achieve crack-free composite film (Supporting Information Figure S2).[43] Furthermore, a toughening agent dibutyl phthalate (DBP) was introduced into the composite film aiming at flexible modification, while the VACNT/Epoxy-DBP film still shows high thermal conductivity of 8.2 W/(m·K) along thickness direction. The flexible film with highly thermal conductivity could be a competitive candidate in advanced thermal management materials.

2. EXPERIMENTAL SECTION

2.1. Materials. Epoxy resin (E44) and polyamide-650 (curing agent) were purchased from Jin Hong rubber industry, China. The epoxide equivalent and softening point of epoxy resin (E44) are 210−244 g/eq and 12−20 °C, respectively. The amine value of polyamide-650 (curing agent) is 220 ± 20 mg KOH/g. Dibutyl phthalate (DBP) was supplied by Chinasun Specialty Products Co., Ltd. Ferrocene and toluene were purchased from Sinopharm Chemical Reagent Co., Ltd., China.

2.2. VACNT Synthesis. VACNTs were grown on silicon wafer via a floating catalyst chemical vapor deposition (FCCVD) method in a quartz tube furnace with the diameter of 3 in.[44,45] The Si wafer was first cut into 3 × 3 cm^2, then put on the quartz plate and push into the middle of the tube furnace. Ferrocene was used as the catalyst and dissolved in toluene with a concentration of 4 wt %. The precursor solution was vaporized at 110 °C before being injected into the furnace along with argon flow ratio of 0.2 L/min. The injection speed of precursor was set to be 5 mL/h by an injection pump (2DMED-201). When the VACNT growth chamber reached 700 °C, the precursor solution was injected into the furnace along with argon flow ratio of 0.4 L/min and hydrogen flow ratio from 0−1 L/min.[46] The growth chamber was kept at 740 °C for 2 h until the VACNT had reached approximately 400 μm in thickness. After cooling down to room temperature, the Si wafer deposited with VACNTs could be taken out.

2.3. Preparation of VACNT/Epoxy Film. Epoxy resin (E44) and polyamide-650 (curing agent) with a mass ratio of 5:4 were mixed completely. Then, the VACNT on silicon wafer was immersed into the mixture and cured in a vacuum oven. The curing temperature was 65 °C and curing time was 4 h. The resulted VACNT/Epoxy composite films were peeled off from the Si wafer substrate. To make sure all CNT tips protruding out of both surfaces, the VACNT/Epoxy composite films were polished to a thickness of 300 μm. We used polishing and burnishing machine (MC004-MP-2) to polish the surface of composite film. The epoxy was much wearproof than CNT arrays during polishing process. By using different sizes of polishing powders (500, 250, and 50 μm) step by step, we were able to obtain smooth polished surfaces. DBP was adopted as a toughening agent in order to improve the flexibility of the composite. The mass fraction of DBP was set to be 20%.

2.4. Characterization. The microstructure and crystallinity of MWCNT was characterized by transmission electron microscopy (TEM, FEI Tecnai G2 F20) and Raman spectroscopy (Raman, Labram HR 800), respectively. Scanning electronic microscope (SEM, Hitachi S4800) was used to observe the morphology of CNT and microstructure of the as-prepared composite. The thermal conductivity of the composite along thickness direction was tested by a Laser flash thermal analyzer (LFA447, NETZSCH) with sample size of Φ12.5 mm. The specific heat capacity of the specimens was obtained by Differential Scanning Calorimeter (DSC, model X). The thermal conductivity (λ) was obtained using the eq 1

$$\lambda(T) = \alpha(T) \times \mathrm{Cp}(T) \times \rho(T) \quad (1)$$

where $\alpha(T)$ is the thermal diffusivity of the sample and $\mathrm{Cp}(T)$ and $\rho(T)$ represent the specific heat capacity and the density of the sample, respectively.

Instron 3365 universal material testing machine was used to test the mechanical performance in z-direction. The films were cut into 15 mm long strips with a width of ∼1 mm, which was precisely measured by an optical microscope. The thickness of the strips were measured by SEM. Mechanical testing was performed on a testing machine (Instron 3365 universal material) with a load cell of 100 N at a displacement rate of 1 mm/min. Elastic property was characterized via the modulus storage changes by Nano Indenter (G200, Agilent Technologies) to confirm the flexibility of the films. The heat dissipation performance was experimentally studied using a Nicolet 6700 FT-IR microscope. The heat reservoir supplied by an electronic heating platform was used to provide a consolidated heat flux for better comparability with silver glue on the surface for 2 × 2 mm^2 buckypaper and VACNT/Epoxy films adhesive. Heat convection and radiation heat transfer impact were elided in this model mainly because of identical carbon nanotube based materials. After heating 15 minutes for samples' thermal stability, thermal infrared images on the both side and lateral surface were taken by the infrared detector to contrast the thermo sensitivity and the heat transfer effect of the carbon-based samples.

3. RESULTS AND DISCUSSION

Aligned arrays were fabricated using a floating catalytic chemical vapor deposition (FCCVD) method as described previously.[44,45] Figure 1a shows a SEM image of representative CNT arrays with height of 400−500 μm, that was used to make composite film. All CNTs are well-aligned and continuous from the bottom to the top, forming a thick CNT forest standing on the silicon wafer. Figure 2a shows typical TEM image of MWCNT in arrays, with the nanotubes typically containing tens of graphitic walls and 65 nm in diameter. Raman spectrum in Figure 2b indicates that the G/D ratio of the nanotubes is ∼2.51. The density of the arrays are measured as high as 0.17 g/cm^3, much higher than the arrays consisting of small diameter nanotubes with density of ∼0.04 g/cm^3 fabricated via catalyst CVD.[47] This high density and large diameter renders the arrays resistive to collapse when they are subjected to high pressure or solution capillary, therefore providing an effective way to prepare crack-free and scalable composite film.

A pre-non-peeled-off silicon wafer process was developed to transfer the aligned CNT into composite film, as described in Figure 1b. First, we prepared samples by embedding the on-wafer aligned CNT arrays in the Epoxy, which is conventionally a type of CNTs composite polymer. The size of composite film depended on the size of CNT arrays, which was scalable and size-controlled by FCCVD fabricated progress. With the CNT

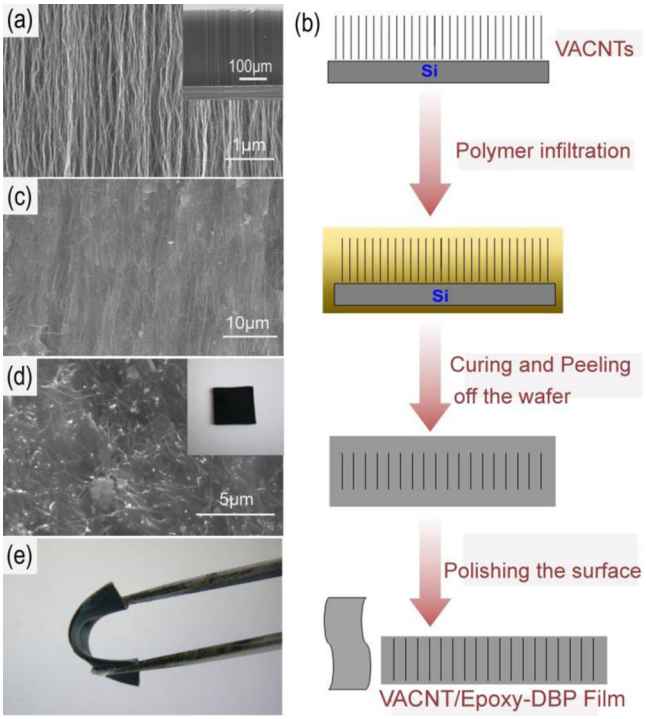

Figure 1. (a) Cross-section SEM image of VACNT morphology (insert image shows VACNT array at low magnification). (b) Schematics of prepared process for VACNT/Epoxy composite film. (c) SEM image by side view of a VACNT/Epoxy film. (d) SEM image by top view of a VACNT/Epoxy film (inserted photograph shows VACNT/Epoxy film at top view). (e) Photograph of VACNT/Epoxy-DBP film at side view being bent with tweezers.

arrays embedded in the Epoxy matrix, the pristine yellowish Epoxy turned black and the outline of the film was almost the same as the original CNT arrays. After cured, the silicon wafer was removed, and the resulting VACNT/Epoxy composites were polished to expose the nanotube tips. This process can efficiently ensure most CNTs remain aligned in the composite film without the occurrence of shrinkage. Figure 1c is a typical side view of the as-prepared composite film, showing the aligned CNTs embedded in the polymer matrix without crack and shrinkage. The CNTs were evidently still aligned in the matrix. Figure 1d is a typical image of top surface of as-prepared composite film, showing most of the CNT tips protruding out of the surface after polishing. The inset in it shows the typical photograph of crack-free VACNT/Epoxy film. With the addition of DBP as a toughening agent, the as-prepared composite film demonstrates good flexibility as shown in Figure 1e.

The thermal conductivity of as-prepared VACNT/Epoxy and VACNT-Epoxy-DBP films were measured and also compared with present reports and buckypapers.[19,32−34] The results are shown in Figure 3. The thermal conductivity of pristine CNT

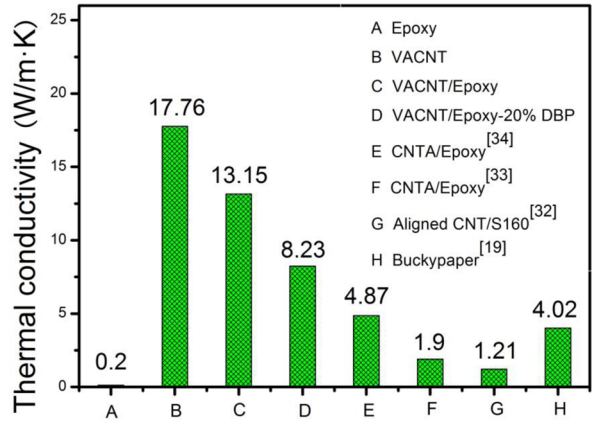

Figure 3. Measured λ (thermal conductivity) of Epoxy (E44), pristine CNT array, VACNT/Epoxy, and VACNT/Epoxy-DBP composite films in thickness of 200 μm compared with reports in the literatures. Indicated E has a 16.7 vol% CNT in Epoxy composite by biaxial mechanical compression with CNT diameter of 8 nm. F was achieved by microwave treatment during composite process to increase in-plane stretching above Tg (the diameter of CNT was 10 nm). G was 0.4 vol % aligned CNT/S160 with diameter of 12 nm. H was the commercial used pure CNT papers (buckypaper, thermal impedance of ~0.27 cm^2·K/W).

arrays with large diameter (~80 nm) was by 17.8 W/(m·K) (indicated by B) and the low-thermal-conductivity Epoxy E44 has a value of 0.20 W/(m·K) (indicated by A). After transfer process, the VACNT/Epoxy film has dramatically maintained a highly thermal conductive by 74.6% with a value of 13.15 W/(m·K) (indicated by C). By complex mechanical compression to increase volume fraction of CNT, Amay et al. has achieved 4.87 W/(m·K) (indicated by E).[34] By a microwave process to increase in-plane stretching, Lin et al. has obtained 1.9 W/(m·K) (indicated by F).[33] Huang et al. prepared a prototype of films using a method called in situ injection molding, by

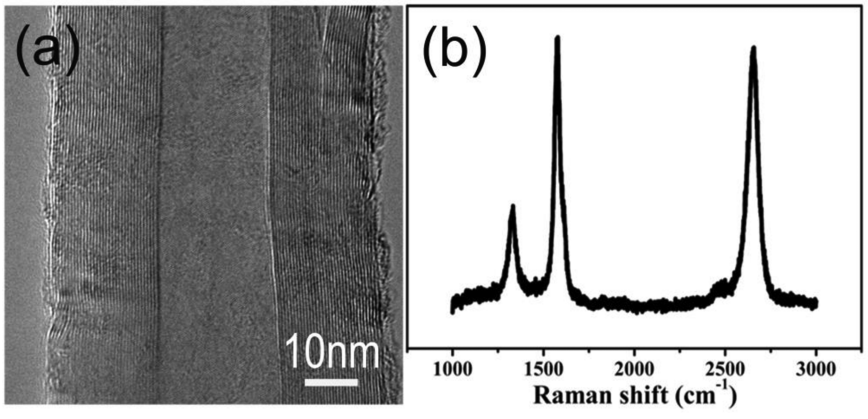

Figure 2. Typical TEM image (a) and Raman spectrum (b) of CNTs by FCCVD.

dx.doi.org/10.1021/am404594m | ACS Appl. Mater. Interfaces 2014, 6, 539−544

embedding aligned CNT arrays in polymer matrix, which showed good thermal conductivity improvements (indicated by G).[32] Obviously, the thermal conductivity was far removed from the pristine CNT arrays. Compared with the E, F and G samples all with smaller CNT diameters and lower thermal conductivity, our larger diameter CNTs has large density of ~0.17 g/cm^3 and robust structure, which was the key issue for keeping the original thermal paths of MWCNTs. By further flexible modification, the thermal conductivity of VACTN/Epoxy-DBP (20 wt %) film is 8.2 W/(m·K), which is almost twice the CNT/Epoxy composite by E. The decrease of thermal conductivity of VACTN/Epoxy-DBP compared to VACTN/Epoxy may be two potential causes. First, DBP has a small molecule segment and lower baseline thermal conductivity, which could significantly reduce the thermal conductivity of polymer matrix. Second, VACNT was embedded in a polymer matrix and discontinuous both in transverse and plane direction, indicating that the heat transfer from the CNT to the polymer matrix worsens with the increase of the DBP percentage because of the poor interface wettability of a thermoplastic toughening agent to CNT.[48] As a result, the DBP agent may sacrifice some part of thermal conductivity meanwhile promoting the application by flexibility. We provide an effective way to transfer the CNT arrays into a freestanding film with highly thermal conductivity and flexibility.

It was also at an advantage than commercial used pure CNT papers (buckypaper, indicated H in Figure 3). Further comparison of the heat dissipation between the VACNT/Epoxy-DBP films and the buckypaper (thermal impedance of ~0.27 cm^2·K/W and thermal conductivity of 4.02 W/(m·K))[19] was performed using infrared imaging technology, as shown in Figure 4a. The side cooling curves from the top to the bottom of the samples are shown in Figure 4b. It can be seen from the surface thermal infrared images (the top right corner in each) that the temperature of buckypaper is about 84−92 °C while the VACNT/Epoxy-DBP film is about 104 °C on the exposure to the same heat source. It is clearly demonstrated that the VACNT/Epoxy film has much better thermal sensitivity for heat transfer than buckypaper. Along the side temperature gradient, the temperature of buckypaper has a gradually dropped line that indicates a modest thermal performance only by thickness of 61 μm. As with the thinner samples, its temperature dropping range is as wide as 25 °C, whereas the VACNT/Epoxy film is just 3 °C with thickness of 204 μm, which leads to the obvious conclusion that the buckypaper is inferior to the VACNT/Epoxy-DBP film in thermal properties.

The VACNT/Epoxy film is at a roughly uniform temperature in nearly its entire, making it able to transmit heat immediately. As we know, a good thermal conductor must be an approximately uniform heat object so that the cold-plate could take away the heat production timely. The excellent heat dispersion display shows the VACNT/Epoxy-DBP film to be a potential candidate as heat conduction material. Furthermore, a clear high-temperature area can be seen above the VACNT/Epoxy-DBP film, which indicates the excellent anisotropy of thermal conductive performance for the introduction of VACNT in the epoxy matrix, whereas there is no such a region seen in the buckypaper.

The mechanical properties of tensile and compress test of the VACNT/Epoxy films with 20 wt % DBP content are shown in Figure 5. The horizontal tensile behavior of VACNT/Epoxy film and VACNT/Epoxy-DBP film are in Figure 5a. The VACNT filler cannot enhance the mechanical performance of

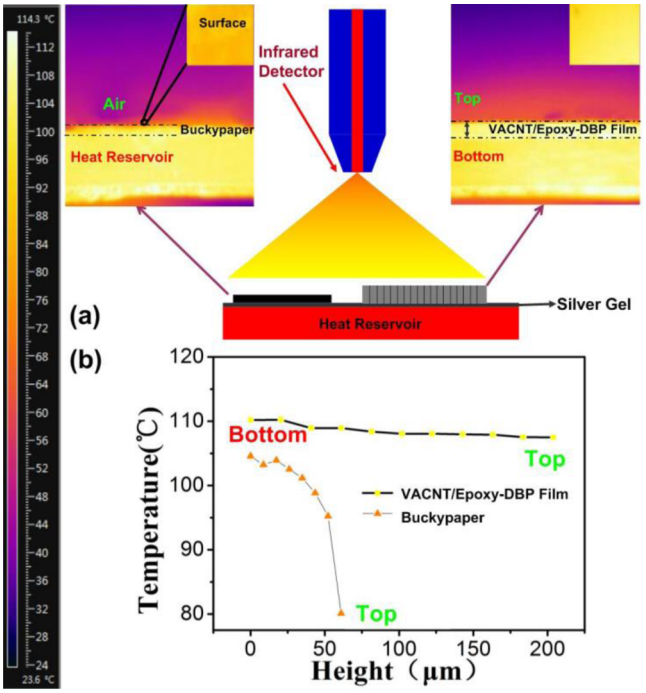

Figure 4. (a) Thermal infrared tested schedule and images for side and surface temperature distribution of buckypaper (in the upper left) and VACNT/Epoxy films (in the upper right). The top right corner insets in each images show the surface temperature, respectively. (b) The compared side cooling curves from bottom to top of VACNT/Epoxy film and buckypaper.

the composite in transverse direction. With the DBP addition, the tensile stress fails and the stretched length increased dramatically because of the flexible reinforcement. The DBP can reduce the viscosity of polymer and improve the interface bond between CNTs and polymer in compositing process (Supporting Information Figure S3), which results in elongation ratio increase significantly from 0.1% to 0.5%. Figure 5b reflects the elastic modification degree with the DBP addition in VACNT/Epoxy films. The storage modulus presents the energy changes in compression process, which generally refers to the elasticity modulus of material. It shows a downward trend in the storage modulus of the composite, which means the addition of DBP makes the composites less rigid, more elastic, and more flexible. It also can be confirmed from Supporting Information Figure S4.

Table 1 summarizes the decomposition temperature and composition proportion of VACNT/Epoxy films (the thermogravimetric analysis (TGA) curve is in Supporting Information, Figure S5). Pure VACNTs are barely decomposed and have little mass loss even at 700 °C in an argon atmosphere, whereas the epoxy resin was almost completely decomposed before 500 °C. For VACNT/Epoxy film, the 300−400 °C decomposition temperature is similar to pure epoxy, and the mass loss is 89.7%, accounting for the total composite material at 700 °C.

After adding DBP, the onset of mass loss appears at 200 °C for DBP decomposition and the second weight loss is the same as pure epoxy resin. The toughening agent introduces a flexible segment in the cross-linking structure of epoxy resin, which could reduce intrinsic modulus of epoxy resin and improve the flexibility. Meanwhile, these segments reduce the density of epoxy polymer and lead to a polymer weight fraction decrease

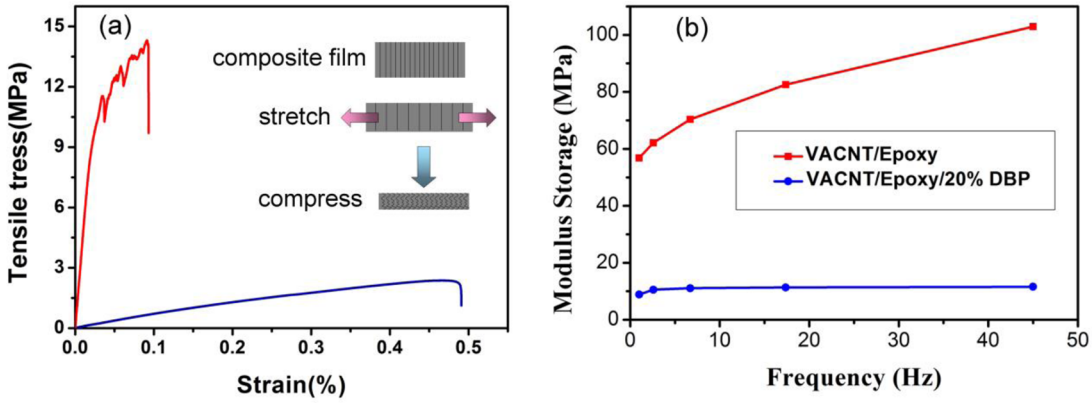

Figure 5. Mechanical properties of VACNT/Epoxy film and VACNT/Epoxy-20 wt %DBP film: (a)The tensile tress and (b) modulus storage in compression (the inset in (a) was tested schematics: the tensile stress was stretched in-plane and the compression test for modulous storage was load cross-plane).

Table 1. VACNT Weight Fraction and Thermal Stability of the Composite Material Estimated from the Thermogravimetric Analysis (TGA) Results

samples	weight loss (%)[a]	weight loss (%)[b]	VACNT fraction wt. %	VACNT fraction vol. %[c]
VACNT	5.25			
Epoxy	16.79	82.21		
VACNT/Epoxy	89.47	89.47	10.53	4.68
VACNT/Epoxy/20% DBP	14.39	68.50	17.11	5.68

[a]Weight loss was measured between 50 and 290 °C. [b]Weight loss was measured between 290 and 700 °C. [c]Density: Epoxy 1.14 g/cm^3; VACNT: 2 g/cm^3.[49]

in VACNT/Epoxy films. Polymers have different degrees of shrinkage after being cured, and the toughening agent, as small molecule segments in intermediate position of the macromolecular chain, caused more sever shrinkage. The degree of polymer contraction, or shrinkage, can be correlated with the percentage of these small molecules, ergo the higher percentage of small molecule segments, the more the polymer contracts. As a result of this shrinkage, the volume fraction of VACNTs increases, but this increase is not enough to compensate for the decline in thermal conductivity caused by DBP. Therefore, it was not contradictory to the decreasing thermal conductivity trend observed in Figure 3.

4. CONCLUSION

In summary, VACNT/Epoxy films were fabricated and investigated for highly thermal conductivity and flexibility. By the transfer of large diameter of MWCNTs under optimized process, a thermal conductivity of 13.2 W/(m·K) was achieved. It has definitely maintained the excellent thermal performance of VACNTs than previous reports for high packing density and good crystalline degree, which provide robust structure to avoid collapse and crack formation during post solution treatment. Adding DBP into epoxy polymer before infusion is an effective way to make composites material infuse better, with a lower void content, and increased flexibility. These crack-free, robust, scalable, flexible, and highly thermally conductive films show promise for applications in the areas of heat transfer and dissipation. Furthermore, the more attention will be paid in the internal heat transfer between CNTs and polymers interface.

■ ASSOCIATED CONTENT

Supporting Information

The photograph of carbon nanotube arrays, SEM image by side view of VACNT/Epoxy film before and after DBP addition, compressive performance and modulus loss (MPa) of VACNT/Epoxy film, TG analysis of VACNT/Epoxy film, and detailed information of thermal conductivity. This material is available free of charge via the Internet at http://pubs.acs.org.

■ AUTHOR INFORMATION

Corresponding Authors

*E-mail: liqiang@mail.njust.edu.cn.
*E-mail: mhchen2008@sinano.ac.cn.
*E-mail: ygyao2013@sinano.ac.cn. Tel: 86-512-62872829. Fax: 86-512-62872552.

Notes

The authors declare no competing financial interest.

■ ACKNOWLEDGMENTS

This work was supported by Natural National Science Foundation of China (No. 51225602 and No. 51372265), the National Basic Research Program (No. 2010CB934700) and the Production and Research Collaborative Innovation Project of Jiangsu Province, China (No. BY2011178). We also acknowledged Dr. Xuefeng Gao for his help of testing infrared thermal image.

■ REFERENCES

(1) Chowdhury, I.; Prasher, R.; Lofgreen, K.; Chrysler, G.; Narasimhan, S.; Mahajan, R.; Koester, D.; Alley, R.; Venkatasubramanian, R. *Nat. Nanotechnol.* **2009**, *4*, 235−238.
(2) Dutta, I.; Raj, R.; Kumar, P.; Chen, T.; Nagaraj, C. M.; Liu, J.; Renavikar, M.; Wakharkar, V. J. J. *Electron. Mater.* **2009**, *38*, 2735−2745.
(3) Carlberg, B.; Wang, T.; Liu, J.; Shangguan, D. *Microelectron. Int.* **2009**, *26*, 28−36.
(4) Fujii, M.; Zhang, X.; Xie, H.; Ago, H.; Takahashi, K.; Ikuta, T.; Abe, H.; Shimizu, T. *Phys. Rev. Lett.* **2005**, *95*, No. 065502.
(5) Pop, E.; Mann, D.; Wang, Q.; Goodson, K.; Dai, H. J. *Nano Lett.* **2006**, *6*, 96−100.
(6) Balandin, A. A. *Nat. Mater.* **2011**, *10*, 569−581.
(7) Yu, C.; Shi, L.; Yao, Z.; Li, D.; Majumdar, A. *Nano Lett.* **2005**, *5*, 1842−1846.
(8) Xu, Y.; Leong, C. K.; Chung, D. D. L. J. *Electron. Mater.* **2007**, *36*, 1181−1187.

(9) Nanda, J.; Maranville, C.; Bollin, S. C.; Sawall, D.; Ohtani, H.; Remillard, J. T.; Ginder, J. M. *J. Phys. Chem.* **2008**, *112*, 654−658.
(10) Bieruck, M. J.; Llaguno, M. C.; Radosalvljevic, M.; Hyun, J. K.; Johnson, A. T.; Fischer, J. E. *Appl. Phys. Lett.* **2002**, *80*, 2767−2769.
(11) Liu, C. H.; Huang, H.; Wu, Y.; Fan, S. S. *Appl. Phys. Lett.* **2004**, *84*, 4248−4250.
(12) Haggenmueller, R.; Guthy, C.; Lukes, J. R.; Fischer, J. E.; Winey, K. I. *Macromolecules* **2007**, *40*, 2417−2421.
(13) Li, Q.; Liu, C.; Fan, S. *Nano Lett.* **2009**, *9*, 3805−3809.
(14) Han, Z.; Fina, A. *Prog. Polym. Sci.* **2011**, *36*, 914−944.
(15) Endo, M.; Muramatsu, H.; Hayashi, T.; Kim, Y. A.; Terrones, M.; Dresselhaus, M. S. *Nature.* **2005**, *433*, 476.
(16) Poggi, M. A.; Lillehei, P. T.; Bottomley, L. A. *Chem. Mater.* **2005**, *17*, 4289−4295.
(17) Gou, J. H. *Polym. Int.* **2006**, *55*, 1283−1288.
(18) Zheng, F.; Baldwin, D. L.; Fifield, L. S., Jr.; Anheier, N. C.; Aardahl, C. L.; Grate, J. W. *Anal. Chem.* **2006**, *78*, 2442−2446.
(19) Chen, H.; Chen, M.; Di, J.; Xu, G.; Li, H.; Li, Q. *J. Phys. Chem.* **2012**, *116*, 3903−3909.
(20) Wang, D.; Song, P.; Liu, C.; Wu, W.; Fan, S. S. *Nanotechnology* **2008**, *19*, No. 075609.
(21) Gonnet, P.; Liang, Z.; Choi, E. S.; Kadambala, R. S.; Zhang, C.; Brooks, J. S.; Wang, B.; Kramer, L. *Curr. Appl. Phys.* **2006**, *6*, 119−122.
(22) Xie, H. J. *Mater. Sci.* **2007**, *42*, 3695−3698.
(23) Aliev, A. E.; Lima, M. H.; Silverman, E. M.; Baughman, R. H. *Nanotechnology* **2010**, *21*, 035709.
(24) Cross, R.; Cola, B. A.; Fisher, T. S.; Xu, X.; Gall, K.; Graham, S. *Nanotechnology* **2010**, *21*, 5705−5713.
(25) Xu, J.; Fisher, T. S. *IEEE Trans. Compon. Packag. Technol.* **2006**, *29*, 261−267.
(26) Panzer, M. A.; Zhang, G.; Mann, D.; Hu, X.; Pop, E.; Dai, H.; Goodson, K. E. J. *J. Heat Transfer* **2008**, *130*, No. 052401.
(27) Maklin, J.; Halonen, N.; Toth, G.; Sapi, A.; Kukovecz, A.; Konya, Z.; Jantunen, H.; Mikkola, J. P.; Kordas, K. *Phys. Status Solidi B* **2011**, *248*, 2508−2511.
(28) Shaikh, S.; Li, L.; Lafdi, K. *Carbon* **2007**, *45*, 2608−2613.
(29) Xie, H.; Cai, A.; Wang, X. *Phys. Lett. A* **2007**, *369*, 120−123.
(30) Akoshima, M.; Hata, K.; Futaba, D. N. *Jpn. J. Appl. Phys.* **2009**, *48*, No. 05EC07.
(31) Yang, D.; Zhang, Q.; Chen, G. *Phys. Lett. A.* **2002**, *329*, 207−213.
(32) Huang, H.; Liu, C.; Wu, Y.; Fan, S. *Adv. Mater.* **2005**, *17*, 1652−1656.
(33) Lin, W.; Moon, K. S.; Wong, C. P. *Adv. Mater.* **2009**, *21*, 2421−2424.
(34) Marconnet, A. M.; Yamamoto, N.; Panzer, M. A.; Wardle, B. L.; Goodson, K. E. *ACS Nano* **2011**, *5*, 4818−4825.
(35) Xu, H. M.; Li, D.; Liang, J. *Chinese J. Inorg. Chem.* **2005**, *21* (9), 1353−1356.
(36) Akoshima, M.; Hata, K.; Futaba, D. N.; Mizuno, K.; Baba, T.; Yumura, M. *Jpn. J. Appl. Phys.* **2009**, *48*, No. 05EC07.
(37) Andrews, R.; Jacques, D.; Rao, A. M.; Derbyshire, F.; Qian, D.; Fan, X.; Dicky, E. C.; Chen, J. *Chem. Phys. Lett.* **1999**, *303*, 467−474.
(38) Chen, L.; Zou, R.; Xia, W.; Liu, Z.; Shang, Y.; Zhu, J.; Wang, Y.; Lin, J.; Xia, D.; Cao, A. *ACS Nano* **2012**, *6*, 10884−10892.
(39) Liu, Z.; Zou, R.; Lin, Z.; Gui, X.; Chen, R.; Lin, J.; Shang, Y.; Cao, A. *Nano Lett.* **2013**, *13*, 4028−4035.
(40) Huang, S.; Li, L.; Yang, Z.; Zhang, L.; Saiyin, H.; Chen, T.; Peng, H. *Adv. Mater.* **2011**, *23*, 4707−4710.
(41) Li, L.; Yang, Z.; Gao, H.; Zhang, H.; Ren, J.; Sun, X.; Chen, T.; Kia, H. G.; Peng, H. *Adv. Mater.* **2011**, *23*, 3730−3735.
(42) Huang, S.; Lin, H.; Qiu, L.; Zhang, L.; Cai, Z.; Chen, T.; Yang, Z.; Yang, S.; Peng, H. *J. Mater. Chem.* **2012**, *22*, 16209−16213.
(43) Sun, X.; Chen, T.; Yang, Z.; Peng, H. *Acc. Chem. Res.* **2013**, *46*, 539−549.
(44) Singh, C.; Shaffer, M. S. P.; Koziol, K. K. K.; Kinloch, I. A.; Windle, A. H. *Chem. Phys. Lett.* **2003**, *372*, 860−865.
(45) Ivanov, I.; Puretzky, A.; Eres, G.; Wang, H.; Pan, Z.; Cui, H.; Jin, R.; Howe, J.; Geohegan, D. B. *Appl. Phys. Lett.* **2006**, *89*, No. 223110.
(46) Zhang, Q.; Huang, J. Q.; Zhao, M. Q.; Qian, W. Z.; Wei, F. *Appl. Phys. A: Mater. Sci. Process.* **2009**, *94*, 853.
(47) Akoshima, M.; Hata, K.; Futaba, D. N.; Mizuno, K.; Baba, T.; Yumura, M. *Jpn. J. Appl. Phys.* **2009**, *48*, No. 05EC07.
(48) Yang, W. P.; Ai, J.; Wang, Q. S. *Mater. Rev.* **2011**, *25*, 394−397.
(49) Bin, Y.; Kitanaka, M.; Zhu, D.; Matsuo, M. *Macromolecules* **2003**, *36*, 6213−6219.